X-Ray Crystallographic Study of Guest–Molecule Orientations in the β-Hydroquinone Clathrates of Acetonitrile and Methyl Isocyanide

Tze-Lock Chan and Thomas C. W. Mak *
Department of Chemistry, The Chinese University of Hong Kong, Shatin, New Territories, Hong Kong

Redetermination of the crystal structure of the Type III β-hydroquinone–acetonitrile clathrate, $3C_6H_4(OH)_2 \cdot CH_3CN$ (1), from new Mo-K_α diffractometer data confirmed the principal finding of previous studies, namely that the three symmetry-independent acetonitrile molecules fit snugly inside clathration cavities in a pseudo-rhombohedral host lattice (space group $P3$), with one guest molecule aligned in the opposite sense to the other two. A parallel study of the potentially isomorphous β-hydroquinone–methyl isocyanide clathrate, $3C_6H_4(OH)_2 \cdot CH_3NC$ (2), showed that it is a Type II clathrate (space group $R3$), in which all three guest molecules in the unit cell are equivalent and point in the same direction parallel to the c axis. The effective molecular length (linear molecular skeleton plus the sum of appropriate van der Waals radii at both ends) of CH_3NC is inferred to be *ca.* 0.1 Å longer than that of CH_3CN, in keeping with the relative stabilities and unit-cell dimensions of (1) and (2). Lattice parameters are: for (1), a = 16.003(2), c = 6.245(2) Å; for (2), a = 15.946(2), c = 6.348(2) Å. The structures have been refined to R values of 0.080 (1) and 0.056 (2) using, respectively, 1 277 and 600 observed reflections.

The structure of the Type III β-hydroquinone–acetonitrile clathrate (1) was determined more than a quarter century ago by Wallwork and Powell [1] from two-dimensional X-ray data. They showed that its trigonal cagework departs from the idealized Type I β-hydroquinone host lattice (space group $R\bar{3}$) [2] which accommodates H_2S and other small guest molecules, and further suggested that one of the three symmetry-independent acetonitrile molecules points in the opposite direction from the other two. These structural features have since been substantiated in a reinvestigation based on three-dimensional film data,[3] and in a recent report on proton-decoupled ^{13}C spectra of the clathrate both as single crystals orientated differently in the magnetic field and as polycrystalline samples spun at the magic angle.[4] The β-hydroquinone–methyl isocyanide (3 : 1) clathrate (2) was first prepared by Davies and Wood,[5] who concluded that it has the same type of host lattice as (1) on the basis of similar hydroquinone Raman bands at *ca.* 470 cm^{-1}. In view of the unique structural relationship between CH_3CN and CH_3NC, we decided to undertake a comparative crystallographic study of (1) and (2). Our objective was three-fold: first, to define more accurately the Type III β-hydroquinone host lattice; second, to determine the preferred orientations of the encaged guest molecules in (2), and hence its structural type; and finally, to compare the relative molecular sizes of CH_3CN and CH_3NC as encageable guest species.

Experimental

Reagent-grade hydroquinone was recrystallized twice from benzene–methanol and dried in a vacuum desiccator. Reagent-grade acetonitrile was used without further purification. Methyl isocyanide was prepared from *N*-methylformamide and toluene-*p*-sulphonyl chloride.[6] The crude product was purified by distillation through a Vigreux column under a stream of nitrogen and the middle 70% fraction, b.p. 60 °C, was collected for use.

Preparation and Handling of $3C_6H_4(OH)_2 \cdot CH_3CN$ (1).—Prismatic crystals were grown by slow evaporation of a saturated solution of hydroquinone in acetonitrile. The clathrate effloresces rapidly in air, and specimens were examined and handled under hexane in a Petri dish. A single crystal of approximate dimensions 0.2 × 0.4 × 0.4 mm was selected and sealed in a 0.5 mm Lindemann glass capillary completely filled with hexane; it remained stable throughout the collection of intensity data.

Preparation and Handling of $3C_6H_4(OH)_2 \cdot CH_3NC$ (2).—Hydroquinone was added to methyl isocyanide with warming in an oil-bath held at 50 °C until saturation was attained. The clathrate deposited on standing at room temperature was retained by decanting off the supernatant and immediately re-dissolved in a minimum amount of fresh, warm methyl isocyanide. Prisms were obtained on further standing. Upon exposure to air, the clathrate instantly turned opaque while emitting a strong smell of methyl isocyanide vapour. Manipulation of the crystals under hexane, in the same manner as for (1), proved troublesome as decomposition was appreciable and became complete within a few hours. After numerous trials, success was achieved by quickly covering a sample fished out of the mother liquor with petroleum jelly. From the resulting slush single crystals were selected and sealed in 0.5 mm Lindemann glass capillaries filled with petroleum jelly. Each freshly mounted crystal lasted for *ca.* 24 h with *ca.* 20% decline in intensity, and two separate crystals were employed in data collection.

Data Collection and Structure Determination.—Accurate unit-cell parameters were obtained from least-squares refinement of 20 high-angle reflections measured on a Nicolet R3m automated four-circle diffractometer with graphite-monochromatized Mo-K_α radiation (λ = 0.710 69A). Intensities were recorded through the range $0° < 2\theta < 55°$ using the ω–2θ scan technique in the bisecting mode. The scan rate varied from 2.0 to 8.0° min^{-1}, with a scan range from 1° below $K_{\alpha 1}$ to 1° above $K_{\alpha 2}$. Background measurement consisted of stationary counts for one-half of the scan time at each end of the scan, and reflections with $I > 1.5\sigma(I)$ were considered observed and used in structure refinement. Three standard reflections were monitored every 50 measurements, and a linear decay correction was made. Information concerning data measurement and structure refinement are summarized in Table 1.

For (1), the asymmetric unit consists of three hydroquinone molecules in general positions and three guest molecules in sites of three-fold rotational symmetry. Refinement commenced with the atomic co-ordinates given in the previous work.[3] The C and O atoms of the host framework were refined anisotropically; by the method of additional observ-

Table 1. Data collection and processing parameters

Compound	(1)	(2)
Formula	$3C_6H_4(OH)_2{\cdot}CH_3CN$	$3C_6H_4(OH)_2{\cdot}CH_3NC$
M	371.38	371.38
Space group	$P3$ ($-h+k+l \neq 3n$ weak or absent)	$R3$
a/Å	16.003(2)	15.946(2)
c/Å	6.245(2)	6.348(2)
U/Å^3	1 385.1(1)	1 397.9(1)
Z	3	3
D_c/g cm^{-3}	1.336	1.323
μ(Mo-K_α)/cm^{-1}	1.12	1.11
Collection range	$\pm h, k, \pm l$	$h, k, \pm l$
Unique data measure	2 144	789
Observed data	1 277	600
No. of variables	236	81
R	0.080	0.053
R_w	0.080	0.075
Goodness of fit S	1.967	1.282

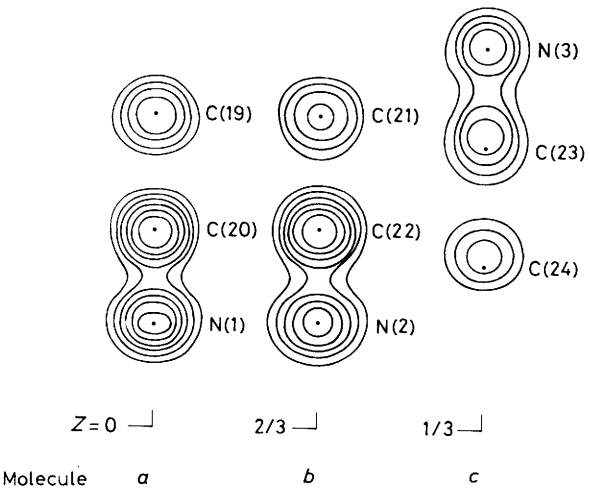

Figure 1. Electron-density sections through the CH_3CN guest molecules a at (0, 0, z_a), b at (1/3, 2/3, $z_b \simeq 2/3 + z_a$), and c at (2/3, 1/3, z_c) in the structure of (1). Contours are drawn at 1 e Å^{-3} intervals starting at 2 e Å^{-3}. For each cage, the dotted line represents the mean plane of its top $[OH]_6$ ring. The disposition of guest molecule c relative to the top $[OH]_6$ ring of its cage is approximately the same as that of molecules a and b with respect to their bottom rings

ational equations,[7,8] interatomic distance constraints of 1.385 ± 0.020 Å * were applied to all C–C and C–O bonds in the three hydroquinone molecules. The non-hydrogen atoms of the CH_3CN guest molecules were varied isotropically, and the aromatic hydrogen atoms were introduced at their calculated positions and allowed to ride on their respective parent carbon atoms, with fixed C–H bond distances (0.96 Å) and isotropic thermal parameters. The resulting difference map clearly showed that the phenolic hydrogen atoms were ordered in the $[OH]_6$ rings; these were included but not varied in subsequent cycles of refinement. The final difference map showed a residual peak of 0.54 e Å^{-3} at 0.36 Å from C(23); all remaining maxima and minima lay between 0.30 and −0.37 e Å^{-3}. Electron-density sections through the three CH_3CN guest molecules are shown in Figure 1.

* A recent survey of structural determination of hydroquinone-containing crystals showed that all C–C and C–O bond lengths in the hydroquinone molecule lay within the range 1.365—1.405 Å.[9]

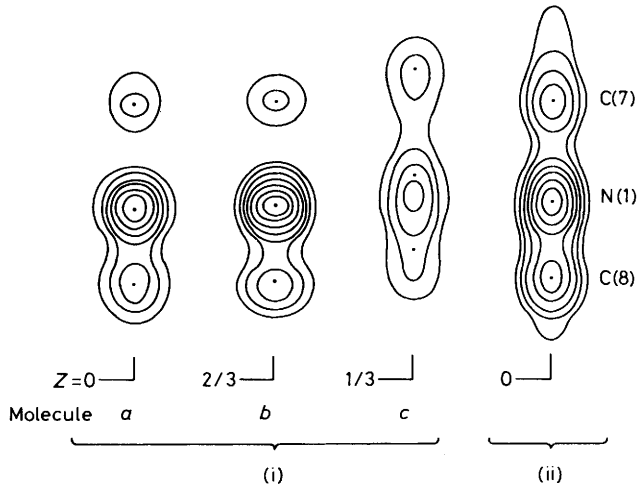

Figure 2. (i) Electron-density sections through three CH_3NC molecules treated as symmetry-independent in the incorrect space group $P3$ for (2). Contours are sketched at 1 e Å^{-3} intervals starting at 2 e Å^{-3}. For each cage, the dotted line represents the mean plane of its top $[OH]_6$ ring. Note that all three guest molecules have the same orientation. (ii) Electron-density section (same contour intervals) through a CH_3NC guest molecule in the correct space group $R3$ for (2). Comparison of (i) and (ii) illustrates the pitfall of refining a structure in an incorrect polar space group of lower symmetry with an unfavourable data-to-parameter ratio

Structure solution of (2) commenced with intensity data collected from four crystals each surviving for a few hours. The space group, either $P3$ or $R3$, could not be uniquely established since many reflections with $-h+k+l \neq 3n$ apparently had intensities significantly greater than $3\sigma(I)$. Initially, the atomic co-ordinates of the host lattice of (1) were refined. A Fourier map gave unequivocal indication that all three CH_3NC guest molecules were similarly orientated along the c axis. Subsequent refinement of (2), proceeding in the same manner as for (1), yielded R 0.080, and electron-density sections suggested that resolution of the atoms in molecule c was rather poor as compared to those in molecules a and b [Figure 2, part (i)]. At this stage intensity data of much better quality became available due to improvement in the method of crystal mounting, making it possible to ascertain that 'weak' reflections with $-h+k+l \neq 3n$ were in fact absent. The true space group for (2) is therefore $R3$, all three guest molecules in the triply primitive hexagonal unit cell being related by translational symmetry. Anisotropic refinement of all 11 non-hydrogen atoms converged at R 0.056, the aromatic and phenolic hydrogen atoms being located and included in structure factor calculations as in the analysis of (1). The final difference Fourier map showed a peak at 0.48 e Å^{-3} in the neighbourhood of atom C(7) of the methyl group; all other maxima and minima were in the range 0.38 and −0.25 e Å^{-3}. A final computation of the electron-density section through a CH_3NC guest molecule yielded clearly resolved peaks [Figure 2, part (ii)].

All computations were carried out on a DGC Nova 3/12 minicomputer with the SHELXTL package of crystallographic programs.[10] Reflection intensities were corrected for

Table 2. Atomic co-ordinates ($\times 10^{-4}$), with standard deviations in parentheses for $3C_6H_4(OH)_2 \cdot CH_3CN$ (1)

	x	*y*	*z*
Guest molecule *a*			
C(19)	0	0	6 294(20)
C(20)	0	0	3 903(15)
N(1)	0	0	2 076(19)
Guest molecule *b*			
C(21)	1/3	2/3	2 947(21)
C(22)	1/3	2/3	633(14)
N(2)	1/3	2/3	−1 203(17)
Guest molecule *c*			
N(3)	2/3	1/3	11 050(19)
C(23)	2/3	1/3	9 003(23)
C(24)	2/3	1/3	6 749(37)
Hydroquinone *a*			
O(1)	1 083(3)	−922(3)	19(6)
C(1)	1 407(4)	−1 275(4)	1 657(9)
C(2)	1 151(6)	−2 233(6)	1 511(13)
C(3)	1 424(5)	−2 646(5)	3 123(11)
C(4)	1 890(4)	−2 124(4)	4 941(9)
C(5)	2 109(5)	−1 163(4)	5 136(8)
C(6)	1 902(5)	−744(5)	3 406(11)
O(2)	2 226(4)	−2 458(4)	6 571(8)
Hydroquinone *b*			
O(3)	4 464(3)	5 774(4)	−3 324(7)
C(7)	4 732(5)	5 388(5)	−1 667(9)
C(8)	4 533(4)	4 466(4)	−1 765(10)
C(9)	4 825(4)	4 048(4)	−226(8)
C(10)	5 279(5)	4 589(5)	1 633(11)
C(11)	5 482(5)	5 553(5)	1 805(11)
C(12)	5 249(4)	5 942(4)	102(9)
O(4)	5 558(3)	4 225(3)	3 303(6)
Hydroquinone *c*			
O(5)	7 750(4)	2 444(4)	3 352(8)
C(13)	8 056(5)	2 078(5)	4 972(10)
C(14)	7 801(4)	1 128(5)	4 981(10)
C(15)	8 099(5)	723(5)	6 455(10)
C(16)	8 622(4)	1 286(4)	8 202(8)
C(17)	8 849(5)	2 253(4)	8 327(11)
C(18)	8 583(4)	2 648(4)	6 672(8)
O(6)	8 913(4)	928(3)	9 885(4)

Table 3. Atomic co-ordinates ($\times 10^{-4}$), with standard deviations in parentheses for $3C_6H_4(OH)_2 \cdot CH_3NC$ (2)

	x	*y*	*z*
Guest molecule			
C(7)	0	0	6 335(34)
N(1)	0	0	4 063(22)
C(8)	0	0	2 378(26)
Hydroquinone			
O(1)	1 107(3)	−908(4)	0 (fixed)
C(1)	1 420(5)	−1 269(5)	1 628(13)
C(2)	1 181(5)	−2 219(4)	1 541(14)
C(3)	1 461(5)	−2 626(5)	3 170(15)
C(4)	1 931(4)	−2 085(4)	4 879(12)
C(5)	2 146(5)	−1 122(5)	5 011(13)
C(6)	1 914(5)	−709(4)	3 408(14)
O(2)	2 218(4)	−2 433(3)	6 554(6)

Table 4. Bond lengths (Å) and bond angles (°) with standard deviations * in parentheses for $3C_6H_4(OH)_2 \cdot CH_3CN$ (1) and $3C_6H_4(OH)_2 \cdot CH_3NC$ (2)

	(1)						(2)	
(*a*) Guest molecules								
C(19)–C(20)	1.493(16)	C(21)–C(22)	1.445(16)	C(23)–C(24)	1.408(27)		C(7)–N(1)	1.442(26)
C(20)–N(1)	1.141(15)	C(22)–N(2)	1.146(14)	N(3)–C(23)	1.278(19)		N(1)–C(8)	1.070(22)
(*b*) Hydroquinone molecules								
O(1)–H(O1)	0.926	O(3)–H(O3)	0.946	O(5)–H(O5)	0.856		O(1)–H(O1)	0.912
O(1)–C(1)	1.388(9)	O(3)–C(7)	1.378(10)	O(5)–C(13)	1.376(10)		O(1)–C(1)	1.391(10)
C(1)–C(2)	1.377(11)	C(7)–C(8)	1.347(11)	C(13)–C(14)	1.363(11)		C(1)–C(2)	1.366(11)
C(2)–C(3)	1.390(13)	C(8)–C(9)	1.379(9)	C(14)–C(15)	1.343(12)		C(2)–C(3)	1.406(13)
C(3)–C(4)	1.386(8)	C(9)–C(10)	1.413(8)	C(15)–C(16)	1.396(8)		C(3)–C(4)	1.355(11)
C(4)–C(5)	1.401(9)	C(10)–C(11)	1.411(11)	C(16)–C(17)	1.403(10)		C(4)–C(5)	1.398(11)
C(5)–C(6)	1.395(11)	C(11)–C(12)	1.375(11)	C(17)–C(18)	1.385(10)		C(5)–C(6)	1.360(13)
C(6)–C(1)	1.367(8)	C(12)–C(7)	1.399(8)	C(18)–C(13)	1.379(8)		C(6)–C(1)	1.411(11)
O(2)–C(4)	1.378(9)	O(4)–C(10)	1.374(9)	O(6)–C(16)	1.385(9)		O(2)–C(4)	1.379(9)
O(2)–H(O2)	0.926	O(4)–H(O4)	0.980	O(6)–H(O6)	0.972		O(2)–H(O2)	0.869
C(1)–O(1)–H(O1)	119	C(7)–O(3)–H(O3)	119	C(13)–O(5)–H(O2)	118		C(1)–O(1)–H(O1)	112
O(1)–C(1)–C(2)	116.1(5)	O(3)–C(7)–C(8)	120.0(5)	O(5)–C(13)–C(14)	120.4(5)		O(1)–C(1)–C(2)	118.0(7)
O(1)–C(1)–C(6)	123.7(7)	O(3)–C(7)–C(12)	121.9(7)	O(5)–C(13)–C(18)	121.0(7)		O(1)–C(1)–C(6)	122.3(8)
C(6)–C(1)–C(2)	120.1(7)	C(12)–C(7)–C(8)	118.0(7)	C(18)–C(13)–C(14)	118.5(7)		C(6)–C(1)–C(2)	119.5(8)
C(1)–C(2)–C(3)	119.5(6)	C(7)–C(8)–C(9)	123.3(5)	C(13)–C(14)–C(15)	124.1(6)		C(1)–C(2)–C(3)	120.3(7)
C(2)–C(3)–C(4)	120.6(7)	C(8)–C(9)–C(10)	118.0(6)	C(14)–C(15)–C(16)	117.8(7)		C(2)–C(3)–C(4)	119.8(7)
C(3)–C(4)–C(5)	119.8(6)	C(9)–C(10)–C(11)	120.0(7)	C(15)–C(16)–C(17)	119.8(7)		C(3)–C(4)–C(5)	120.1(7)
C(4)–C(5)–C(6)	118.1(5)	C(10)–C(11)–C(12)	118.0(6)	C(16)–C(17)–C(18)	119.5(6)		C(4)–C(5)–C(6)	120.7(7)
C(5)–C(6)–C(1)	121.6(7)	C(11)–C(12)–C(7)	122.2(7)	C(17)–C(18)–C(13)	119.9(6)		C(5)–C(6)–C(1)	119.5(7)
O(2)–C(4)–C(3)	124.6(6)	O(4)–C(10)–C(9)	122.6(6)	O(6)–C(16)–C(15)	122.9(6)		O(2)–C(4)–C(3)	123.4(6)
O(2)–C(4)–C(5)	115.4(5)	O(4)–C(10)–C(11)	117.3(6)	O(6)–C(16)–C(17)	117.3(5)		O(2)–C(4)–C(5)	116.6(6)
C(4)–O(2)–H(O2)	108	C(10)–O(4)–H(O4)	108	C(16)–O(6)–H(O6)	114		C(4)–O(2)–H(O2)	112

* Standard deviations for bond distances and angles involving phenolic H atoms are not listed since they were not varied in least-squares refinement.

Table 5. Interatomic distances (Å) and bond angles (°) in hydrogen-bonded $[OH]_6$ rings, and close guest–host van der Waals contacts (Å) *

(*a*) Hydrogen bonding in $3C_6H_4(OH)_2{\cdot}CH_3CN$ (1) †

(i) Cage A centred at (0, 0, $z \sim \frac{1}{2}$), z of O(1) − z of O(6)^{I} = 0.0134

O(1) · · · O(6)^{I}	2.792	O(6)^{II} · · · O(1) · · · O(6)^{I}	120.4
O(1) · · · O(6)^{II}	2.788	O(1) · · · O(6)^{I} · · · O(1)^{III}	119.5

(ii) Cage B centred at (1/3, 2/3, $z \sim 1/6$), z of O(3) − z of O(2)^{IV} = 0.0105

O(3) · · · O(2)^{IV}	2.785	O(2)^{II} · · · O(3) · · · O(2)^{IV}	117.9
O(3) · · · O(2)^{II}	2.782	O(3) · · · O(2)^{IV} · · · O(3)^{V}	121.9

(iii) Cage C centred at (2/3, 1/3, $z \sim 5/6$), z of O(5) − z of O(4)^{VI} = 0.0049

O(5) · · · O(4)^{VI}	2.745	O(4)^{VII} · · · O(5) · · · O(4)^{VI}	121.4
O(5) · · · O(4)^{VII}	2.773	O(5) · · · O(4)^{VI} · · · O(5)^{VII}	118.6

(*b*) Close guest–host interactions in (1) †

C(19) · · · O(1)^{VIII}	3.63	N(1) · · · O(1)	3.07
C(19) · · · O(6)^{IX}	3.58	N(1) · · · O(6)^{X}	3.11
C(19) · · · N(1)^{VIII}	3.61		
C(21) · · · O(2)^{XI}	3.57	N(2) · · · O(2)^{XII}	3.09
C(21) · · · O(3)^{VIII}	3.65	N(2) · · · O(3)	3.11
C(21) · · · N(2)^{VIII}	3.65		
C(24) · · · O(5)	3.46	N(3) · · · O(5)^{VIII}	3.11
C(24) · · · O(4)	3.51	N(3) · · · O(4)^{VIII}	3.09
C(24) · · · N(3)^{XIII}	3.56		

(*c*) Hydrogen bonding in $3C_6H_4(OH)_2{\cdot}CH_3NC$ (2) ‡

Cage centred at (0, 0, $z \sim \frac{1}{2}$), z of O(1) − z of O(2)^{I} = 0.0113

O(1) · · · O(2)^{I}	2.779	O(2)^{II} · · · O(1) · · · O(2)^{I}	120.0
O(1) · · · O(2)^{II}	2.800	O(1) · · · O(2)^{I} · · · O(1)^{III}	119.9

(*d*) Close guest–host interactions in (2) ‡

C(7) · · · O(1)^{IV}	3.63	C(8) · · · O(1)	3.17
C(7) · · · O(2)^{V}	3.59	C(8) · · · O(2)^{VI}	3.21

* Estimated standard deviations for individual O · · · O hydrogen bonds, O · · · O · · · O angles, and guest–host contacts are 0.006 Å, 0.3°, and 0.01 Å, respectively.

Symmetry code:

† I $-y, -1 + x - y, -1 + z$; II $1 - x + y, 1 - x, -1 + z$; III $-x + y, -x, z$; IV $-y, x - y, -1 + z$; V $-x + y, 1 - x, z$; VI $1 - y, x - y, z$; VII $1 - x + y, 1 - x, z$; VIII $x, y, 1 + z$; IX $-1 + x, y, z$; X $-1 + x, y, -1 + z$; XI $x, 1 + y, z$; XII $x, 1 + y, -1 + z$; XIII $x, y, -1 + z$

‡ I $-1/3 - y, -2/3 + x - y, -2/3 + z$; II $2/3 - x + y, 1/3 - x, -2/3 + z$; III $-x + y, -x, z$; IV $x, y, 1 + z$; V $-1/3 + x, 1/3 + y, 1/3 + z$; VI $-1/3 + x, 1/3 + y, -2/3 + z$

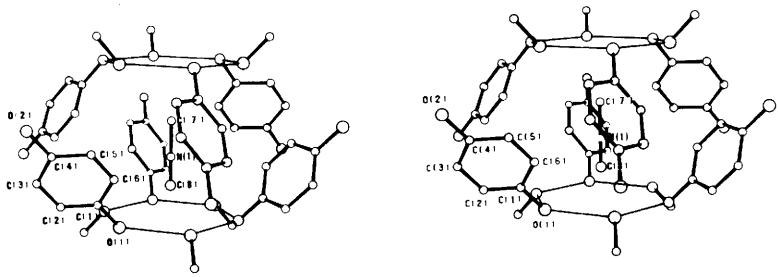

Figure 3. Stereodrawing showing a CH_3NC guest molecule trapped inside a cage in the structure of (2). For clarity all hydrogen atoms have been omitted. The labelled atoms correspond to the positional parameters in Table 3

Lorentz and polarization effects but not for absorption. Analytical expressions [11] of complex atomic scattering factors [12] were used. The weighting scheme employed for the blocked-cascade least-squares refinement and analysis of variance was $w = [\sigma^2(F) + 0.0005|F|^2]^{-1}$. The weighted discrepancy factor and goodness-of-fit parameter are defined as $R_w \equiv [\Sigma w(\Delta F)^2/\Sigma w(F_o)^2]^{\frac{1}{2}}$ and $S \equiv [\Sigma w(\Delta F)^2/(m - n)]^{\frac{1}{2}}$ (where m = number of observed reflections and n = number of variables), respectively.

The final positional parameters for the non-hydrogen atoms in the two structures are given in Tables 2 and 3; atom labelling generally follows the scheme of ref. 3, with

appropriate changes for the CH_3NC guest molecule in (2) (Figure 3). Bond distances and angles are presented in Table 4. Table 5 lists hydrogen-bond distances and angles as well as close guest–host van der Waals interactions. Thermal parameters, hydrogen co-ordinates, and observed and calculated structure factors are in Supplementary Publication No. SUP 23546 (19 pp.).*

Discussion

Refinement of the structure of the Type III β-hydroquinone–acetonitrile (3 : 1) clathrate (1) confirmed all principal findings of the previous study,[3] namely that the three symmetry-independent acetonitrile molecules fit snugly inside clathration cavities in a pseudo-rhombohedral host lattice (space group *P*3), with one guest molecule orientated in the opposite sense to the other two. The improved precision may be seen by comparing Figure 1 with the corresponding Figure in ref. 3. Somewhat unexpectedly, the β-hydroquinone–methyl isocyanide (3 : 1) clathrate (2) turned out to have a Type II structure (space group *R*3) in which all three guest molecules in the unit cell are equivalent and hence aligned in the same sense. The structure of (2) is thus isomorphous with those of the HCl [13] and CH_3OH [14] clathrates, except that the latter two guest species interact more strongly, most likely due to hydrogen bonding, with the walls of their respective clathration cavities.

The fact that CH_3CN and CH_3NC, both prolate spherical tops and isoelectronic, should yield β-hydroquinone clathrates which deviate from isomorphism seems intriguing. Microwave spectroscopy has shown that the linear molecular skeleton of CH_3CN [CH_3–C 1.468(2), C≡N 1.159(2) Å] [15] is slightly longer, by *ca.* 0.04 Å, than that of CH_3NC [CH_3–N 1.424(2), N≡C 1.166(2) Å],[16] yet in host–guest packing one should instead consider their relative 'effective molecular lengths,' taking into account the sum of the appropriate van der Waals radii at both ends of each molecule. Since both molecules have the same methyl group at one end, they differ only in the nature of the terminal atom at the other. With estimates of the van der Waals radius of C in the range 1.65—1.70 Å [17,18] weighed against commonly accepted values of 1.50—1.55 Å for N, the effective molecular length of CH_3NC may very well exceed that of CH_3CN by *ca.* 0.1 Å. In accord with this expectation, (2) is much less stable than (1), the unit cell of (2) is significantly greater than that of (1), and the *c* and *a* axes of (2) are longer and shorter, respectively, than the corresponding values of (1). Taken together, these data indicate that accommodation of the sterically more demanding CH_3NC guest molecules stretches the β-hydroquinone host lattice to its limit in the *c* direction. The instability of (2) in air can be rationalized in terms of a strong drive for guest escape to relieve tension in a host lattice close to breaking point, and coating the crystals with petroleum jelly slows down the decomposition process by partially blocking the escape routes.

Both CH_3CN and CH_3NC are highly polar molecules, the former with an electric dipole moment of 3.56 D in benzene.[19] The dipole moment of CH_3NC is not readily available, but may be estimated as *ca.* 4.0 D from the known data for C_2H_5CN (3.55 D in benzene) and C_2H_5NC (4.01 D in the vapour).[20] In the crystal structures of (1) and (2), the polar guest molecules adopt a head-to-tail columnar arrangement parallel to *c* and normal to the $[OH]_6$ rings. The available data indicate that the shorter CH_3CN molecules are less rigidly held than the CH_3NC molecules in their respective clathration cavities, with a larger lateral inter-columnar spacing in (1) (by *ca.* 0.03 Å) as compared with (2). These very slight nuances, in addition to the greater dissimilarity in the dipole moments of CH_3CN and CH_3NC, should be taken into account in any subtle explanation of the different guest-molecule orientations in (1) and (2).

In both clathrates the C_6O_2 skeleton of each hydroquinone molecule is planar within experimental error, and the C–C–O angles (Table 4) exhibit the well established inequality due to the steric effects of the phenolic H atoms.[9] The hydrogen-bonded $[OH]_6$ rings deviate slightly but significantly from exact planarity (Table 5). Each $[OH]_6$ ring has an ordered proton arrangement, and the O–H . . . O(H) distances (Table 5) in (1) and (2) are significantly longer than the average values of 2.700, 2.70, and 2.716 Å for corresponding hydrogen bonds in the Type I H_2S,[2] Type II HCl,[13] and Type II CH_3OH [14] β-hydroquinone clathrates.

An alternative classification of β-hydroquinone clathrates into three types, based on the splitting patterns of the host-lattice Raman bands in the 470 cm^{-1} region, has been proposed by Davies and Wood.[5] Unfortunately there seems to be no useful correlation between this and the crystallographic criterion adopted in our work. For instance, the HCl, CH_3OH, and CH_3NC clathrates exhibit very distinct host-lattice Raman spectra, yet all belong to space group *R*3. On the other hand, although the CH_3CN clathrate has the same splitting pattern of the Raman bands as the CH_3NC clathrate, it crystallizes in space group *P*3 and constitutes the only authenticated example to date of a Type III β-hydroquinone clathrate.

References

1 S. C. Wallwork and H. M. Powell, *J. Chem. Soc.*, 1956, 4855.
2 T. C. W. Mak, J. S. Tse, C. Tse, K. Lee, and Y. Chong, *J. Chem. Soc., Perkin Trans. 2*, 1976, 1169.
3 T. C. W. Mak and K. Lee, *Acta Crystallogr., Sect. B*, 1978, **34**, 3631.
4 J. A. Ripmeester, J. S. Tse, and D. W. Davidson, *Chem. Phys. Lett.*, 1982, **86**, 428.
5 J. E. D. Davies and W. J. Wood, *J. Chem. Soc., Dalton Trans.*, 1975, 674.
6 R. E. Schuster, J. E. Scott, and J. Casanova, *Org. Synth.*, 1966, **46**, 75.
7 J. Waser, *Acta Crystallogr.*, 1963, **16**, 1091.
8 J. S. Rollett, in 'Crystallographic Computing,' ed. F. R. Ahmed, Munksgaard, Copenhagen, 1969, pp. 169—172.
9 S. C. Wallwork and H. M. Powell, *J. Chem. Soc., Perkin Trans. 2*, 1980, 641.
10 G. M. Sheldrick, SHELXTL User Manual, Revision 3, Nicolet XRD Corporation, Cupertino, 1981.
11 D. T. Cromer and J. B. Mann, *Acta Crystallogr., Sect. A*, 1968, **24**, 321.
12 'International Tables for X-ray Crystallography,' Kynoch Press, Birmingham, 1974, vol. 4, pp. 55, 99, 149.
13 J. C. A. Boeyens and J. A. Pretorius, *Acta Crystallogr., Sect. B*, 1977, **33**, 2120.
14 T. C. W. Mak, *J. Chem. Soc., Perkin Trans. 2*, 1982, 1435.
15 K. Karakida, T. Fukuyama, and K. Kuchitu, *Bull. Chem. Soc. Jpn.*, 1974, **47**, 299.
16 C. C. Costain, *J. Chem. Phys.*, 1958, **29**, 864.
17 A. Bondi, *J. Phys. Chem.*, 1964, **68**, 441.
18 N. L. Allinger, J. A. Hirsch, M. A. Miller, I. J. Tyminski, and F. A. Van-Catledge, *J. Am. Chem. Soc.*, 1968, **90**, 1199.
19 A. L. McClellan, 'Tables of Experimental Dipole Moments,' Rahara Enterprises, El Cerrito, 1974, vol. 2, p. 54.
20 Ref. 19, p. 78.

* For details see Notices to Authors No. 7, *J. Chem. Soc., Perkin Trans. 2*, 1981, Index Issue.

Received 25*th June* 1982; *Paper* 2/1066